Heliyon 10 (2024) e32813

Contents lists available at ScienceDirect

Heliyon

journal homepage: www.cell.com/heliyon

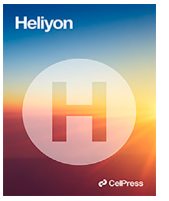

Research article

Large-amplitude plasma wave generation by laser beating in inhomogeneous magnetized plasmas

Motahareh Arefnia [a], Mohammad Ghorbanalilu [a,*], Ali Reza Niknam [b]

[a] Department of Physics, Shahid Beheshti University, Tehran, Iran
[b] Laser and Plasma Research Institute, Shahid Beheshti University, Tehran, Iran

ARTICLE INFO

Keywords:
Beatwave excitation
Linear-radial density profile
Quadratic-radial density profile
Electron acceleration
External magnetic field

ABSTRACT

Large-amplitude plasma wave is known to accelerate electrons to high energies. The electron energy gain mainly depends on plasma wave amplitude. In this paper, we investigate the excitation of large-amplitude plasma waves by laser beat-wave in an inhomogeneous plasma. The idea behind this work is to employ linear and radial plasma density profiles to enhance the plasma wave amplitude. PIC simulations are used to validate the numerical solution of the nonlinear wave equation in cylindrical dimensions through the finite difference method. Furthermore, the effects of the quadratic-radial plasma density profiles and magnetic field on the plasma wave excitation are investigated. The study shows that compared to the linear density profile of plasma, the plasma wave amplitude in the case of a linear-radial density profile is far more pronounced. For the linear-radial density profile, the plasma wave amplitude remains steady over greater distances of propagation compared to the linear density profile, resulting in reduced immediate damping effects. It can also be seen that the plasma wave amplitude is higher for the quadratic-radial than for the linear-radial density profiles. The effect of a longitudinal magnetic field on plasma wave amplitude is investigated. It can be seen that the plasma wave amplitude is increased by applying a magnetic field. This study may provide a way to enhance the plasma wave field for accelerating the electrons in laser-plasma accelerators.

1. Introduction

The exploration of plasma wakefield accelerator (PWFA) [1–4], plasma beat wave accelerator (PBWA) [5,6], laser wakefield accelerator (LWFA) [7–12], and self-modulated laser wakefield accelerators [13] involves the use of high-energy laser pulses to interact with plasmas in order to accelerate charged particles. Laser wakefield accelerators offer various possibilities for applications, including generating X-ray radiation, producing harmonics, and achieving high-gradient particle acceleration [14–18]. Exciting plasma waves is a proposed method for accelerating electrons, as explored in many studies [19–25]. Rosenbluth and Liu were the first to propose a plasma beat wave accelerator (PBWA) that does not require high-power lasers [5,26,27]. The modulation of laser beams occurs when two laser pulses, each with slightly different wavelengths, are directed into plasma, resulting in the generation of a longitudinal ponderomotive force. When the beat and plasma frequencies are in alignment, the ponderomotive force resonantly excites a plasmon, leading to the heating of electrons to multiple electron volts. Because the longitudinal plasmon phase velocity in an underdense plasma with $\omega_{1,2} >> \omega_p$ (where $\omega_{1,2}$ denotes the laser beam frequencies and ω_p denotes the plasma frequency) is

* Corresponding author.
E-mail address: m_alilu@sbu.ac.ir (M. Ghorbanalilu).

https://doi.org/10.1016/j.heliyon.2024.e32813
Received 10 January 2024; Received in revised form 9 June 2024; Accepted 10 June 2024

Available online 14 June 2024

nearly equivalent to the speed of light in plasma [28–30]. Even the weakly relativistic laser pulse in PBWA generates a big amplitude electric field [31]. In PBWA and LWFA, the amplitude of the electric field can fluctuate to over one Gigaelectronvolt (> 1 GeV); yet, the energy transferred to the plasma electrons is constrained by the diffraction length of the laser pulse [32,33].

To avoid laser beam diffraction and enhance the acceleration distance in laser-plasma setups, optical guiding can be utilized to extend the propagation range by multiple Rayleigh lengths [34–36]. Optical guiding is achieved through preformed density channels, relativistic self-focusing, and plasma waveguiding, allowing for increased propagation distances [37,38]. By utilizing a preformed plasma waveguide, diffraction can be restricted for a specific laser power, resulting in higher energy gains [39]. The quiver motion of heavy electrons causes the refraction index to decrease with increasing intensity in relativistic self-focusing [40–42]. Various plasma channel configurations, including parabolic, tapered, and hollow channels, have been previously studied for acceleration driven by high-gradient lasers [43–45]. Wakefields can be generated using a plasma channel with a parabolic density profile, where the density of electrons on the axis is consistent, typically denoted as n_0, but peaks gradually with radius [46]. The effect of external magnetic field and self-generated magnetic field on harmonic generation [47], self-focusing of the laser pulse [48], wakefield excitation and electron acceleration [49] is clearly significant. Another widely studied form of plasma channel is the hollow channel, in which wakefields are generated along the channel walls. Therefore, in the highly relativistic regime, when beams travel along the central axis, the longitudinal field and the transverse dimension behave independently, causing the transverse field to become negligible [50]. In contrast to a hollow channel where the axial field is decoupled from the transverse direction and particles absorb energy uniformly, parabolic plasma channels have minimal density along the central axis, and the gradient index is influenced by the radial profile. Employing corrugated plasma channels in laser wakefield acceleration appears to be a promising solution for overcoming the dephasing constraint. Two-dimensional (2D) particle-in-cell (PIC) simulations exhibit quasi-phase-matching in an axially-modulated plasma waveguide, revealing an increase in the transverse wakefield with the radial position [51].

In this study, the plasma wave is generated through the nonlinear interaction of two laser beams beating in an inhomogeneous plasma. The model presented in this paper is aimed at extending plasma wave amplitude by considering the plasma density profile as a quadratic-radial. We introduce the plasma wave equation for the linear-radial plasma density profile, which is derived from the momentum conservation equation combined with the Maxwell equations. First, we briefly review the plasma wave excitation in the plasma with the linear density profile, which was solved analytically using the Airy function [5]. Then, we apply the fourth-order Runge-Kutta method (RK4) to solve the plasma wave equation in the plasma and compare results with analytical results. Since the main challenge in acceleration is to achieve large amplitudes of the plasma waves, our main idea is to increase the plasma amplitude by evolving the plasma density as a linear-radial density profile. For improving the plasma wave field, we also consider the plasma density profile as quadratic-radial instead of linear-radial. Beyond that, for increasing the propagation distance of the plasma wave, we assume the background plasma to be inhomogeneous with the quadratic-radial density profile. Hence, we employ the finite difference method (FDM) for solving the nonlinear wave equation in a plasma channel by considering the linear-radial and expanding to the quadratic-radial density profile to model the plasma wave excitation by beating laser beams. Our results reveal that in the plasma channel with a linear-radial density profile, the plasma wave extends over a longer propagation distance than in the case of a linear plasma density profile. Moreover, the plasma wave amplitude in quadratic-radial is higher than the linear-radial density profile. Furthermore, the effect of the longitudinal magnetic field on plasma wave amplitude is considered. The PIC simulation has been employed to describe plasma wave by beating two laser beams in a quadratic-radial density profile. Our simulation results show using an external magnetic field to increase plasma wave plays an important role in improving acceleration gradient. Here, the acceleration gradient for the quadratic-radial density profile can reach around 3 GV/m. However, in the case of magnetized plasma, the electron acceleration gradient can reach 6 GV/m.

The paper is organized in the following way. In Sec. 2, we provide a concise overview of the analytical solution for exciting the plasma wave through the beating of two laser beams in a plasma with a linear density profile as described by Rosenbluth and Liu [5], then we bring our numerical results and compare them with analytical solutions. In Sec. 3, we describe the suggested scheme of linear-radial density profile for large-amplitude plasma wave excitation and present a numerical method to solve the new plasma wave equation, then we expand the method for the quadratic-radial density profile. The PIC simulation aspect and the longitudinal magnetic field applied to the suggested scheme are described in Sec. 4. A conclusion of the results is presented in Sec. 5.

2. Plasma wave excitation with linear plasma density profile

2.1. Analytical solution

Consider two linearly polarized laser beams of frequencies ω_1 and ω_2, wave numbers k_1 and k_2 co-propagating along the z-direction in an inhomogeneous plasma with the linear density profile of $n(z) = n_0(1 + z/L)$. Considering the dispersion relation ($\omega^2 = \omega_p^2 + 3k^2v_e^2$), a plasma wave's phase velocity slows down as it enters a region of decreasing density (increasing $k(z)$). This slowing down can lead to Landau damping when the phase velocity approaches the thermal speed of the particles. In cases with minimal density variation, the wave vector $k(z)$ can be approximated as constant for a basic understanding of this phenomenon. The frequency of the lasers is assumed to be much higher than the electron plasma frequency and ion motion is neglected. The momentum transfer equation in the presence of two electromagnetic plane waves $\mathbf{E}_{1,2} = \hat{y}E_{1,2}sin(k_{1,2}z - \omega_{1,2}t)$ where $E_{1,2}$ are the field amplitude of the laser beams, is as follows:

$$\frac{\partial \mathbf{v}}{\partial t} = -\frac{\nabla p}{mn} - (\mathbf{v}.\nabla)\mathbf{v} + \frac{e}{m}(\mathbf{E} + \frac{\mathbf{v}}{c} \times \mathbf{B}), \tag{1}$$

where **v**, e, and m are the velocity, charge, and mass of electrons, respectively. p, and **E** denote the electron pressure and the electric field within the plasma. To generate the plasma wave, the plasma temperature (T) must be above zero. For a gas obeying ideal behavior, pressure is $p = Cn^{\gamma}$ whereas $\gamma = 3$ in the case of an adiabatic process where C is constant. The following equation is obtained for the electrostatic field by the linearized Fourier-component of momentum transfer equation and the Poisson equation $\partial E/\partial t = -4\pi n_0 e v_z$,

$$\frac{\partial^2 E}{\partial z^2} - \frac{\omega_0^2 z}{3v_e^2 L} E = \left(-\frac{i}{12}\frac{e}{m}\frac{\omega_p^2(z)\Delta k}{\omega_1\omega_2 v_e^2} E_1 E_2^*\right) e^{-i\Delta k z}, \tag{2}$$

where $\omega_0 = \Delta\omega = \omega_1 - \omega_2$, $\Delta k = k_1 - k_2$, $v_e = \sqrt{K_B T/m}$ and $\omega_p(z) = \sqrt{4\pi e^2 n(z)/m}$ refer to the electron thermal velocity and plasma frequency, respectively. Eq. (2) is a nonhomogeneous ordinary differential equation (ODE) that is solved by the known Airy-equation in two special cases when $z \to \infty$ and $z \to -\infty$. In the first case, the wave is damped, and in the second, the Green's function method is used to determine the plasma wave's field:

$$\begin{aligned} E(-\infty) = {} & \pi^{1/2}\left(\frac{\alpha}{|z|}\right)^{1/4} \exp\left(\frac{-2}{3} i\alpha^{1/2}|z|^{3/2} - i\frac{\pi}{4}\right) \\ & \times -\frac{i}{4}\frac{e}{m}\frac{\omega_p^2(z)\Delta k L}{\omega_1\omega_2\omega_0^2} E_1 E_2^* \exp\frac{i\Delta k^3 v_e^2 L}{\omega_0^2} + E_-(-\infty), \end{aligned} \tag{3}$$

where $\alpha = \omega_0^2/3v_e^2 L$ and $E_-(-\infty) = \pi^{1/2}(\alpha/|z|)^{1/4} \exp\left(-2i\alpha^{1/2}|z|^{3/2}/3 - i\pi/4\right)$.

2.2. Numerical solution

Due to the complexity and asymptotic nature of the analytical solution, we outline the numerical approach for solving the plasma wave equation and subsequently compare our findings with the analytical solution. The RK4 method discretizes the approximate solutions of the nonlinear ordinary differential equations presented in Eq. (2). Since the wave equation represents a second-order ordinary differential equation, a development of the RK4 method is necessary to facilitate the solution of the plasma wave. This issue is elucidated briefly in the following description. Consider the 2nd-order ODE (Eq. (2)) as

$$\frac{dE}{dz} - C_1 z E = F(z), \tag{4}$$

where, $C_1 = \omega_0^2/3v_e^2 L$, and $F(z) = (-ie\omega_p^2(z)\Delta k E_1 E_2^*/12m\omega_1\omega_2 v_e^2) e^{-i\Delta k z}$. Subject to the initial conditions, $E(z = -0.4\text{ cm}) \approx 0.1$, $dE/dz \approx -0.02$. The second-order ordinary differential equation can be transformed into a pair of first-order ODEs by introducing the following variables.

$$W_1 = E, \qquad W_2 = \frac{dE}{dz}, \tag{5}$$

with initial conditions (in $z = -0.4$) $W_1 = 0.1$ and $W_2 = -0.02$. The variable substitution $W_2 = dE/dz$ is equivalent to

$$\frac{dW_1}{dz} = W_2, \tag{6}$$

while the ODE is re-written as

$$\frac{dW_2}{dz} - C_1 z W_1 = F(z), \tag{7}$$

and is solved by the Euler method with a step size of $h = 0.5$ μm($\approx \lambda_1/21$). Detailed descriptions of this method can be obtained in the reference list [52].

To investigate the plasma wave excitation in a plasma with the linear density profile, the wave amplitude is plotted for the following laser and plasma parameters. Plasma waves driven by CO_2 lasers have operating parameters of $\lambda_1 = 10.6$ μm and $\lambda_2 = 10.3$ μm. The normalized amplitude in the non-relativistic regime is $a_0 << 1$, where $a_0^2 = 7.3 \times 10^{-19}[\lambda(\mu\text{m})]^2 I_0(\text{W/cm}^2)$ with laser intensity $I_0 = 10^{14}$ W/cm^2. Laser beams can produce an electric field with an amplitude at about $E_{1,2} = 2.7 \times 10^8$ V/cm. The electron temperature is $T = 10$ keV, plasma length is $L = 0.4$ cm, and initial density is $n_0 \approx 10^{16}$ cm^{-3}. The plasma wave electric field can increase to a high value in the linear regime. A simple estimate for the maximum field assumes all of the plasma electrons are oscillating, where $E_{max} = E_{WB}$, and $E_{WB}[\text{V/cm}] \approx 0.96 n^{1/2}[\text{cm}^{-3}]$ is the non-relativistic wave-breaking field. Hence, we normalize the plasma wave amplitude by the maximum wave breaking. A comparison between the analytical and numerical solutions of the plasma wave is presented in Fig. 1. These plots exhibit a similar oscillating structure of the plasma wave in the plasma with the linear density profile. The peak amplitude of the electrostatic waves increases as it approaches the resonance condition ($z \approx 0$ and $\omega_1 - \omega_2 \approx \omega_p$), as illustrated in Fig. 1. A visual representation in Fig. 1 shows how a plasma wave oscillates as the resonance condition weakens.

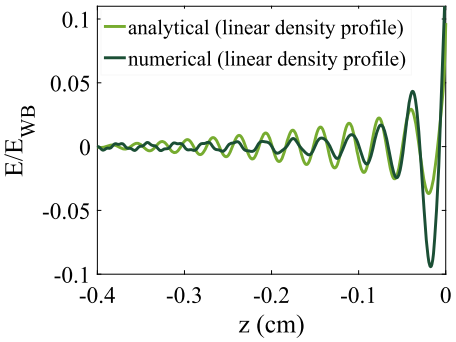

Fig. 1. The sketches of the plasma wave pattern considering linear plasma density profile in terms of propagation distance. Comparison of numerical and analytical solutions.

3. Numerical results and analysis

3.1. Plasma wave excitation in the linear-radial plasma density profile

In this section, we consider a modified structure of the plasma density profile i.e., a linear-radial density profile, $n(z,r) = n_0(1 + z/L + \delta n r^2/n_0 r_{ch}^2)$, where the density perturbation is denoted by δn, which is small compared to n_0, and r_{ch} represents the channel radius. We get the wave equation as follows by applying a system of Maxwell and hydrodynamic equations to determine the plasma wave's excitation:

$$\frac{1}{r}\frac{\partial E}{\partial r} + \frac{\partial^2 E}{\partial r^2} + \frac{\partial^2 E}{\partial z^2} - \frac{4\pi e^2}{3v_e^2 m}(n(r,z) - n_0)E \quad = S(r,z), \tag{8}$$

where $S(r,z) = (-ie\omega_p^2(r,z)\Delta k E_1 E_2^*/12m\omega_1\omega_2 v_e^2)e^{-i\Delta kz}$. Eq. (8) is a nonhomogeneous partial differential equation (PDE) that displays the plasma channel's plasma wave field. The analytical solution of Eq. (8) was obtained asymptotically using the hypergeometric functions in cylindrical geometry [53]. Here, we demonstrate the numerical approach for solving the nonlinear wave equation (Eq. (8)), which is implemented in the discrete framework of the finite difference method (FDM). The discretization of the plasma channel applies to the non-rectangular region, and it's independent of ϕ. Taylor's series expansion approach is applied to the implementation of the obtained physical model. This technique employs cylindrical coordinates (r, ϕ, z) with discrete size steps $(\Delta z, \Delta r, \Delta\phi)$ defined by a step size h. ϕ is not needed because an axisymmetric system is a specific example ($E = E(r,z)$). It is assumed that the finite difference grid of an axisymmetric system, with $\Delta r = \Delta z = h$. The computation region has a total size of 40000 cells and a step size of $h = 0.5$ μm($\approx \lambda_1/21$). For more details on the FDM method, please refer to reference number [54].

Solving the plasma wave equation with the FDM method and considering the boundary conditions gives us the electrostatic field. Given a long plasma channel with length L and radius r_{ch}, the plasma wave equation (Eq. (8)) takes the following form:

$$\frac{\partial^2 E}{\partial r^2} + \frac{1}{r}\frac{\partial E}{\partial r} + \frac{\partial E}{\partial z^2} - (C_1 z + C_2 r^2)E = S(r,z), \tag{9}$$

where, $C_2 = \omega_0^2\delta n/3v_e^2 n_0 r_{ch}^2$. In this cylindrical part of the grid, we use a special method (second-order centered finite difference stencils) to approximate how the values change in the direction of the radius.

$$\begin{aligned} E(I,J) = \frac{1}{4 + G(I,J)} + \Big(&\frac{2J+1}{2J}E(I,J+1)\frac{2J-1}{2J}E(I,J-1) + E(I+1,J) \\ &+ E(I-1,J) - C_3(H(I,J))\Big), \end{aligned} \tag{10}$$

where, $z = Ih$, $r = Jh$, $G(I,J) = Ih^3C_1 + J^2h^4C_2$, $C_3 = -ie\omega_0^2\Delta k E_1 E_2^*/12m\omega_1\omega_2 v_e^2$, $H(I,J) = (h^2 + Ih^3/L + \delta nJ^2h^4/n_0 r_{ch}^2)e^{-i\Delta kIh}$. To solve the plasma wave equation numerically, we create a grid with points in both the axial (z direction, N_z points) and radial (r direction, N_r points) directions. The circular boundary's field is as

$$E(I,J) = \frac{1}{2 + M(I,J)}\Big(E(I+1,J) + E(I-1,J) - C_3 e^{-I\Delta kIh}\Big), \tag{11}$$

where, $M(I,J) = Ih^3C_1$. Due to the symmetry of the channel, there is a singularity in $r = 0$ where by using $\frac{\partial E}{\partial r}|_{r=0} = 0$ we can obtain

$$E(I,J) = \frac{1}{6 + G(I,J)}\Big(4E(I,1) + E(I+1,0) + E(I-1,0)\Big). \tag{12}$$

Therefore, using Eqs. (10), (11), (12) the plasma wave equation (Eq. (8)) in a plasma channel can be solved.

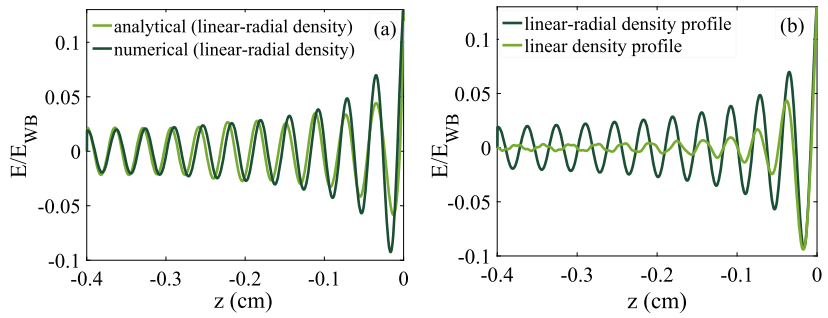

Fig. 2. (**a**) Comparison of the plasma wave equation's numerical and analytical solutions in a linear-radial plasma density profile. Variations in the normalized amplitude plasma wave with respect to distance in $r = 50$ μm, $r_{ch} = 100$ μm, $\delta n = 0.2n_0$, with more variables like those in Fig. 1. (**b**) Comparison of plasma wave amplitude with two density profiles: linear and linear-radial plasma density profile. Normalized amplitude of the plasma wave as a function of propagation distance from the numerical perspective using parameters similar to Fig. 1.

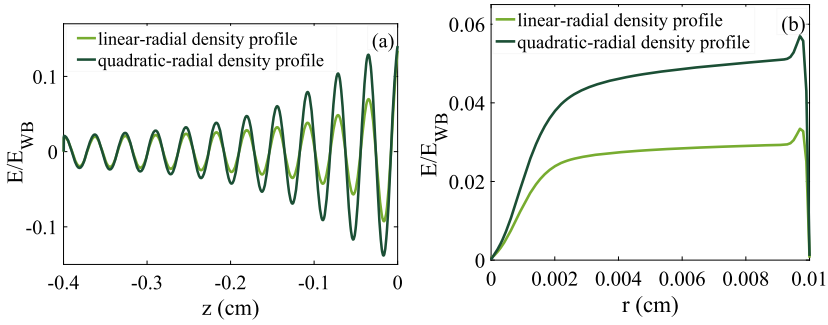

Fig. 3. (a) Normalized plasma wave amplitude as the propagation distance in the background of linear-radial and quadratic-radial, $r = 50$ μm. (**b**) Normalized plasma wave amplitude as the plasma channel radius for linear-radial and quadratic-radial density profiles, for distance almost in the middle of the plasma channel, parameters are similar to Fig. 2.

3.2. Impact of density profiles (linear vs. linear-radial) on plasma waves

Fig. 2a compares numerical solutions (FDM) with analytical solutions from prior work [53] to validate the numerical approach for the plasma wave equation with a linear-radial density profile. We can further analyze the impact of density profiles by comparing the wave amplitudes obtained numerically for linear and linear-radial profiles (shown Fig. 2b). Fig. 2a gives appropriate agreement between the plasma wave amplitude in the plasma channel, both analytically and numerically solved (Eq. (9)), the parameters remain identical to those shown in Fig. 1. As shown in Fig. 2b, the amplitude of the plasma wave is higher and more stable in the plasma with the linear-radial density profile than the linear density profile. It is intuitively understood that the plasma density reduction for $z < 0$ is very smooth for the linear-radial density profile due to the channel effect, so we expect the excited plasma wave to experience slow damping compared to the linear density profile. As a result, we can claim that this is an advantage and greater significance for wakefield excitation by beating waves in the plasma channel.

3.3. Quadratic-radial density profile

We improve the proposed modification of the plasma density profiles as quadratic-radial density profile ($n(r,z) = n_0(1 - z^2/L^2) + \delta n r^2/r_{ch}^2$) to achieve much larger plasma wave amplitudes. While a perfectly quadratic plasma density profile may be challenging, various techniques offer controlled, non-uniform profiles. These include tapered capillaries, differential gas feeding, magnetic confinement, laser ablation, and plasma channels, allowing for tailored density manipulation [55–59]. Fig. 3a compares the plasma wave amplitude for a quadratic-linear background electron density profile in a long, thin cylindrical simulation region. As we can see in Fig. 3a, the plasma wave amplitude is higher for the quadratic-radial profile, than for the linear-radial density profile. Fig. 3b plots the radial dependence of the plasma wave amplitude for both density profiles, using the same parameters as Fig. 3a. It is clear from the figure, the plasma wave amplitude for the quadratic-radial profile is greater than the linear-radial profiles. In addition, the plasma wave amplitude for the quadratic-radial profile increases much more with channel radius compared to the linear-radial profile. As expected, the presence of a plasma channel leads to a significantly stronger plasma wave. It is evident that the amplitude of the plasma wave is affected by the radius of the channel. For radial variation, we see a relatively sharp increase near the wall of the channel.

In this section, we discussed the advantage of the linear-radial density profile over a linear profile in the plasma wave excitation from long laser wavelengths. We also proposed the quadratic-radial density profile to achieve large plasma wave amplitude and following that, improved electron acceleration. Research suggests the plasma wave within the channel behaves similarly to the

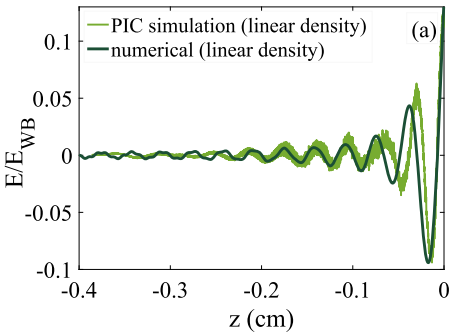

Fig. 4. Comparison of the numerical, and 1D-simulation solutions (t = 15 ps) in an inhomogeneous plasma with a linear density profile. Variations of the normalized amplitude of the plasma wave in terms of propagation distance, with parameters similar to Fig. 1.

wakefield produced by lasers interacting with corrugated plasma channels [51]. PBWA uses two low-powered lasers to create a beating effect that excites strong plasma waves, trapping and accelerating electrons to high energies [60]. Notably, recent studies have explored various techniques to optimize particle acceleration through beatwave interaction. These techniques include controlling the phase velocity of the plasma wakefield ([61]) and auto-resonant phase-locking ([62]). We now investigate how test electrons are accelerated by the excited plasma wave within the channel. Guiding laser pulses through plasma is considered a key method for achieving longer particle acceleration distances. High-energy electron acceleration is possible with a plasma wave if the laser pulses spread widely without diffraction. Particles trapped in the wave's acceleration zone gain momentum, moving faster in the same direction as the wave. Matching the wave's phase velocity allows particles to gain energy as they travel alongside it. Similar to achieving 0.7 GV/m acceleration with a weakly nonlinear CO_2 laser, a two-frequency CO_2 laser can also excite a resonant plasma wave with the same acceleration gradient [63,64]. This study investigates the potential for enhanced electron acceleration using beatwave interaction within a plasma channel. Our results reveal that the achievable electron acceleration gradient reaches approximately 1 GV/m in a standard plasma channel. However, by employing a specifically designed quadratic plasma channel, the electron acceleration gradient significantly increases, exceeding 3 GV/m. This substantial enhancement demonstrates the effectiveness of the quadratic channel geometry in optimizing electron acceleration through the beatwave interaction.

This research investigates a promising approach for manipulating plasma waves. These profiles offer significant advantages over traditional uniform shapes. Creating the desired quadratic-radial plasma profile can be achieved using existing techniques. Pre-plasmas involve pre-ionizing a channel with the desired density variation before the main interaction. Methods like capillary discharges or tailored laser pulses (as referenced by [65]) can be used for this purpose. External channeling structures physically guide the plasma using tools like dielectric capillaries or magnetic confinement. These structures influence the plasma shape and can potentially achieve the required quadratic-radial profile [66,67]. These established techniques offer a practical path for realizing the proposed profile.

4. Plasma wave excitation in the presence of an external magnetic field: PIC simulation results

In what follows, we present the results of PIC simulations to validate the theoretical model discussed in the previous sections. We confirm that the outcomes of the PIC simulation are consistent with previous analytical and numerical findings. The influence of a magnetic field on laser wakefield acceleration has already been considered in several works [12,68,69]. This research uses PIC simulation to examine the impact of a strong magnetic field on the plasma wave excitation amplitude caused by laser beating. The PIC simulations employ the 2D and 1D EPOCH codes [70] to model the generation of plasma waves through the interaction of two CO_2 laser beams. The laser beams are linearly polarized with wavelengths of 10.6 μm and 10.3 μm. In the 1D simulation, we considered a linear regime where laser beams with an intensity of $I = 10^{14}$ W/cm^2 excited plasma waves through a linear ($n(z) = 1 + z/L$) and quadratic ($n(z) = 1 - z^2/L^2$) plasma density profiles. The longitudinal length of the plasma is 4000 μm. Furthermore, 2D simulations are conducted using a plasma with the linear-radial and quadratic-radial density distributions, denoted as $n(r, z)$. The simulation box has dimensions of 4000 μm in the longitudinal direction and 220 μm in the radial direction, with spatial resolutions of 0.2 μm($\approx \lambda_1/50$) and 2.75 μm($\approx \lambda_1/4$), respectively. The duration of both simulations (1D and 2D) was set to be longer than the beating time in the plasma, specifically $t = 15$ ps.

Fig. 4 displays the results of the 1D simulation with the linear density profile. We compare these simulation results with the numerical solutions. The plasma wave field is of the same order obtained from the numerical solutions and both results are in good agreement. Notably, as the resonance conditions are approached, the amplitude of the plasma wave increases, reaching its peak at the resonance point ($z \approx 0$).

We show 2D PIC simulation results for plasma wave excitation in Figs. 5(a, b). The plots illustrate the plasma wave field resulting from the two lasers beating. However the including of radial density increases the plasma frequency and slightly decreases the plasma wave amplitude in the resonance region, but it causes the large amplitude for plasma wave away from the resonance point. The maximum amplitude of the plasma wave field is almost the same as obtained from the numerical model. The PIC simulation results are reasonably in agreement with the theoretical results, however, some differences may be there in comparison with the

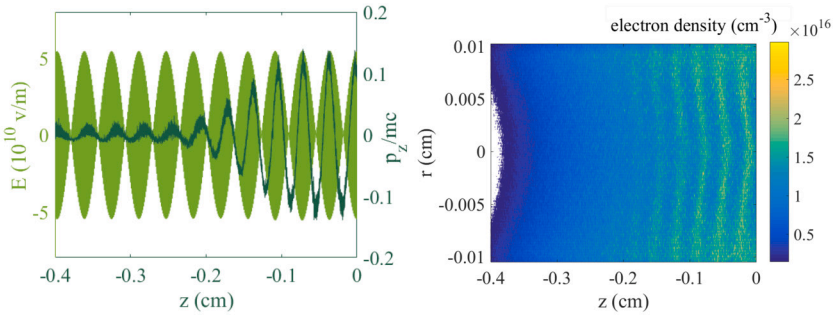

Fig. 5. (**a**) Electron phase space plot with electric fields of a 2D PIC simulation at $t = 15$ ps for quadratic-radial density profile ($\delta n/n_0 = 0.2$). The momentum is normalized to electron mass times the speed of light on the right y-axis (P_z/mc) (Dark green). The electric field representing the laser (laser evolution) indicated by the propagation distance (light green) left y-axis ($E(10^{10}$ V/m)). (**b**) Contour plot of the electron density based plasma channel radius in terms of propagation distance for quadratic-radial density profile in $t = 15$ ps with parameters similar to Fig. 2.

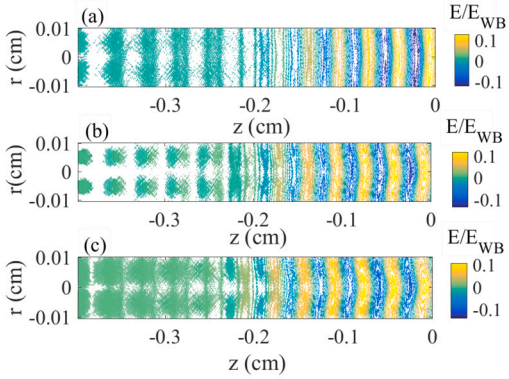

Fig. 6. Contour plot of the normalized plasma wave amplitude of based plasma channel radius in terms of propagation distance for quadratic-radial density profile in t = 15 ps for (**a**) $\delta n/n_0 = 0.1$, (**b**) $\delta n/n_0 = 0.2$, (**c**) $\delta n/n_0 = 0.25$ with parameters similar to Fig. 2.

theoretical investigation. We believe that this difference could be due to the finite transverse size of the plasma in the simulations or the slight difference in the density profiles as the PIC simulation has a higher-order polynomial representation of the density profile.

Fig. 5a (light green), provides a framework for explaining a plot that depicts a periodic evolution of laser intensity in a beatwave interaction. Here, the periodicity arises due to the combined effects of two lasers with different frequencies. The period of the oscillation in the plot is directly linked to the difference in frequencies ($\triangle\omega$) between the two lasers. A larger frequency difference will result in a shorter period (faster oscillations) on the plot. Fig. 5a (dark green), presents a phase space plot, specifically focusing on the normalized momentum (p/mc) of electrons on the z-axis plotted against the propagation distance. It visualizes how the momentum of electrons changes as they travel through the plasma due to the influence of the propagating wave. Fig. 5b presents a contour plot depicting the evolution of the electron density within a plasma channel. The x-axis represents the propagation distance for a wave and beat traveling through the plasma and the y-axis represents the radial distance from the center of the channel. The specific density profile used in this case is quadratic-radial. The wake structure exploited for particle acceleration techniques like laser wakefield acceleration. The high electric field associated with the density gradient within the wake is used to accelerate electrons to high energies. Analyzing the wake structure helps to understand the efficiency of the acceleration process.

The results of PIC simulation for plasma wave excitation by beat wave laser beams in quadratic-radial density are plotted by different combinations of beatwaves. However the laser beam's strength is weak ($a_0 = eE/mc\omega << 1$), beat wave arising from the interference of two beams can be very strong. The normalized amplitude is proportional to the laser field intensity and wavelength as $a_0^2 \simeq 7.3 \times 10^{-19}[\lambda(\mu\text{m})]^2 I_0(\text{W/cm}^2)$. The figure shows that increasing the amplitude of two laser beams causes to increase in the beatwave amplitude and as a result much strong plasma wave. It is clear from the contour plots of Figs. 6(a-c) and Figs. 7(a-c) that the plasma wave field is optimized by the development of parameters of plasma density and laser.

The momentum transfer equation for electrons is modified to incorporate the Lorentz force due to an external magnetic field (B_0), accounting for its influence on electron motion.

$$\frac{\partial \mathbf{v}}{\partial t} = -\frac{\nabla p}{mn} - (\mathbf{v}.\nabla)\mathbf{v} + \frac{e}{m}(\mathbf{E} + \frac{\mathbf{v}}{c} \times (\mathbf{B} + \mathbf{B}_0)). \tag{13}$$

The resonance condition is $\omega_0 = k v_{ph}(z = 0) \pm \omega_c$, where, $\omega_c = eB/m_0$ is the cyclotron frequency. While we don't directly calculate the phase velocity (v_{ph}) using PIC simulations in this specific instance, their value lies in capturing the comprehensive dynamics of the plasma, including wave propagation even in the presence of an external magnetic field (B_0). The concept of excitation of the

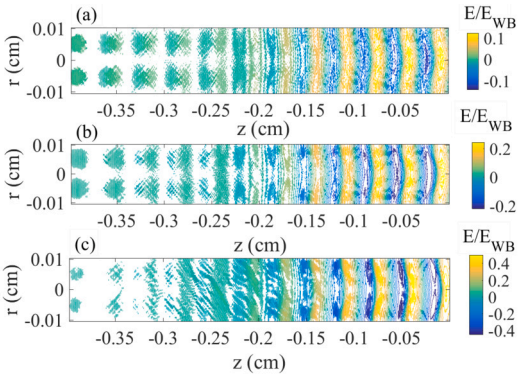

Fig. 7. Contour plot of the normalized plasma wave amplitude based plasma channel radius in terms of propagation distance for quadratic-radial density profile in $t = 15$ ps for (**a**) $a_{01} = 0.09, a_{02} = 0.088$, (**b**) $a_{01} = 0.128, a_{02} = 0.124$, (**c**) $a_{01} = 0.181, a_{02} = 0.176$ with parameters similar to Fig. 2.

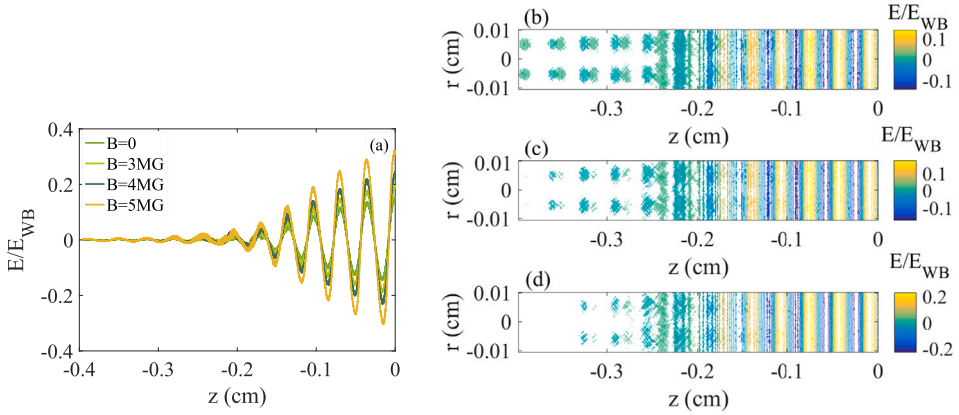

Fig. 8. (**a**) Comparison of the non-magnetized, and magnetized simulation solutions ($t = 15$ ps) in a quadratic density profile. Variations of the normalized amplitude of the plasma wave in terms of propagation distance, with parameters similar to Fig. 1. Contour plot of the normalized plasma wave amplitude based plasma channel radius in terms of propagation distance for quadratic-radial density profile in $t = 15$ ps for (**b**) B = 3 MG, (**c**) B = 4 MG, (**d**) B = 5 MG with parameters similar to Fig. 2.

plasma wave is further clarified in Fig. 8a displays the impact of varying magnetic field strengths on the plasma with a quadratic density profile. The figure illustrates that the peak amplitude of the wave increases in the presence of a magnetic field, and as the magnetic field is increased, the amplitude of the plasma wave also rises. Figs. 8(b-d) compare the wave amplitude peaks created by the beating of laser beams for non-magnetized plasma and plasma in the presence of longitudinal magnetic fields. Our work offers distinct advantages over the study by Razavinia et al. ([12]), who investigated laser wakefield excitation in a magnetized plasma slab using a one-dimensional relativistic Vlasov-Maxwell model. While their work demonstrated the potential of magnetic fields to enhance wakefield amplitude, our approach achieves a significantly greater increase using a lower magnetic field strength ($B = 500$ T) in combination with optimized density profiles (linear-radial or quadratic-radial). Though conventional magnets have difficulty reaching kilotesla fields, laser-driven coils utilizing intense laser pulses have successfully achieved this milestone. This novel technique shows great potential for creating controllable, ultra-strong magnetic fields [71]. The existence of an external magnetic field confines the electrons at the wavefront of the plasma wave, therefore, the coupling with the plasma wave improved over a long distance. A magnetic field also limits free-streaming by forcing particles to gyrate in Larmor orbits. Since the Larmor radius of the particle orbit decreases as the magnetic field increases, the radius of curvature of the orbit is smaller in the regions of the stronger B field. This can lead to enhanced particle motion, affecting plasma wave behavior.

5. Conclusions

We investigated a way to excite high-amplitude electron plasma waves by beating two lasers in an inhomogeneous plasma. The numerical solution of the plasma wave field was obtained and validated by PIC simulations. We reviewed the analytical solution of the plasma wave field driven by the laser beating in the plasma with linear and linear-radial density profiles. Numerical results were presented and compared for two solutions of the plasma wave equation for the case of linear and linear-radial plasma density profiles. Furthermore, FDM was applied to obtain the plasma wave amplitude by beatwave excitation in the quadratic-radial density profiles. The findings indicated that the plasma wave amplitude is greater and more consistent in the linear-radial density profile compared to the linear density profile. However, the plasma wave amplitude is damped in a linear density profile after a short

distance from the resonance point. It was shown that the plasma wave amplitude could be enhanced in the quadratic and quadratic-radial density profiles compared to the plasma wave amplitude in the linear and linear-radial density profiles. Furthermore, the presence of a magnetic field causes an enhancement of the plasma wave amplitude. This growth of plasma wave amplitude causes an increase in the acceleration of the electrons. In this method, the linear-radial profile allows electron acceleration by plasma beat waves to achieve 1 GV/m; in contrast, the linear plasma density profile showed substantially weaker electron acceleration. Our results indicated electron acceleration in the quadratic-radial density profile can reach 3 GV/m. The PIC simulation results also confirmed these findings. The plasma wave amplitude attains a two-fold enhancement due to the magnetic field. According to our PIC simulation, electron acceleration and plasma wave amplitude were improved up to 6 GV/m by beatwave activation for quadratic-radial density profile in the presence of a longitudinal magnetic field. Overall, the presence of a longitudinal magnetic field can significantly influence the behavior of plasma waves through various mechanisms, ultimately contributing to the strengthening of the waves. Therefore, the plasma wave field amplitude will depend on the characteristics of the plasma, the magnetic field strength, and other relevant parameters.

CRediT authorship contribution statement

Motahareh Arefnia: Writing – original draft, Investigation, Data curation. **Mohammad Ghorbanalilu:** Writing – review & editing, Supervision, Project administration, Investigation. **Ali Reza Niknam:** Writing – review & editing.

Declaration of competing interest

The authors declare the following financial interests/personal relationships which may be considered as potential competing interests: Mohammad Ghorbanalilu reports a relationship with Department of physics, Shahid Beheshti University that includes: employment. If there are other authors, they declare that they have no known competing financial interests or personal relationships that could have appeared to influence the work reported in this paper.

Data availability

The datasets generated during and/or analyzed during the current study are available from the corresponding author on reasonable request.

Acknowledgements

The authors gratefully acknowledge the valuable contribution of Suho Kim, Chunghwa Lee, the guidance and support of Prof. D. N. Gupta, and the provision of access to the essential computational resources by the High-Performance Computing at the Gwangju Institute of Science and Technology (GIST) of South Korea.

References

[1] J.B. Rosenzweig, B. Breizman, T. Katsouleas, et al., Acceleration and focusing of electrons in two-dimensional nonlinear plasma wake fields, Phys. Rev. A 44 (10) (1991) R6189.
[2] R. Roussel, G. Andonian, W. Lynn, et al., Single shot characterization of high transformer ratio wakefields in nonlinear plasma acceleration, Phys. Rev. Lett. 124 (4) (2020) 044802.
[3] S. Barzegar, M. Sedaghat, A.R. Niknam, Controlled electron injection into beam driven plasma wakefield accelerators employing a co-propagating laser pulse, Plasma Phys. Control. Fusion 63 (12) (2021) 125016.
[4] D.N. Gupta, S.R. Yoffe, A. Jain, et al., Propagation of intense laser pulses in plasma with a prepared phase-space distribution, Sci. Rep. 12 (1) (2022) 20368.
[5] M.N. Rosenbluth, C.S. Liu, Excitation of plasma waves by two laser beams, Phys. Rev. Lett. 29 (11) (1972) 701.
[6] R.J. Noble, Plasma-wave generation in the beat-wave accelerator, Phys. Rev. A 32 (1) (1985) 460.
[7] T. Tajima, J.M. Dawson, Laser electron accelerator, Phys. Rev. Lett. 43 (4) (1979) 267.
[8] F. Amiranoff, S. Baton, D. Bernard, et al., Observation of laser wakefield acceleration of electrons, Phys. Rev. Lett. 81 (5) (1998) 995.
[9] M. Rezaei-Pandari, A.R. Niknam, R. Massudi, et al., Wakefield evolution and electron acceleration in interaction of frequency-chirped laser pulse with inhomogeneous, Phys. Plasmas 24 (2) (2017) 023112.
[10] M. Mirzaie, G. Zhang, S. Li, et al., Effect of injection-gas concentration on the electron beam quality from a laser-plasma accelerator, Phys. Plasmas 25 (4) (2018) 043106.
[11] Z. Jin, K. Nakamura, N. Pathak, et al., Coupling effects in multistage laser wake-field acceleration of electrons, Sci. Rep. 9 (1) (2019) 20045.
[12] S.N. Razavinia, M. Ghorbanalilu, Effect of external magnetic field on wakefield generation in underdense plasma slab using backward semi-Lagrangian Vlasov code, Phys. Rev. Accel. Beams 22 (11) (2019) 111305.
[13] N. Hafz, M.S. Hur, G.H. Kim, et al., Quasimonoenergetic electron beam generation by using a pinholelike collimator in a self-modulated laser wakefield acceleration, Phys. Rev. E 73 (1) (2019) 016405.
[14] H.M. Milchberg, C.G. Durfee, et al., Application of a plasma waveguide to soft-x-ray lasers, Opt. Soc. Am. B 12 (4) (1995) 731–737.
[15] B. Shokri, M. Ghorbanalilu, Parametric instability of plasmas produced by linearly polarized microwave pulsed fields, Phys. Plasmas 12 (4) (2005) 043506.
[16] R.P. Sharma, P.K. Chauhan, Nonparaxial theory of cross-focusing of two laser beams and its effects on plasma wave excitation and particle acceleration: relativistic case, Phys. Plasmas 15 (6) (2008) 063103.
[17] G. Purohit, P. Rawat, R. Gauniyal, Second harmonic generation by self-focusing of intense hollow Gaussian laser beam in collisionless plasma, Phys. Plasmas 23 (1) (2016) 013103.
[18] A. Jain, D.N. Gupta, Optimization of electron bunch quality using a chirped laser pulse in laser wakefield acceleration, Phys. Rev. Accel. Beams 24 (11) (2021) 111302.

[19] G. Shvets, J.S. Wurtele, T.C. Chiou, et al., Excitation of accelerating wakefields in inhomogeneous plasmas, IEEE Trans. Plasma Sci. 24 (2) (1996) 351–362.
[20] J. Osterhoff, A. Popp, Zs. Major, et al., Generation of stable, low-divergence electron beams by laser-wakefield acceleration in a steady-state-flow gas cell, Phys. Rev. Lett. 101 (8) (2008) 085002.
[21] A. Debus, R. Pausch, A. Huebl, et al., Circumventing the dephasing and depletion limits of laser-wakefield acceleration, Phys. Rev. X 9 (3) (2019) 031044.
[22] M. Rezaei-Pandari, F. Jahangiri, A.R. Niknam, Optimizing the electron acceleration in vacuum by chirped ultrashort laser pulse using particle swarm method, Laser Part. Beams 37 (3) (2019) 242–251.
[23] S.N. Razavinia, M. Ghorbanalilu, Semi-Lagrangian Vlasov simulation of the interaction between femtosecond chirped and double laser pulses with a thin plasma slab, Plasma Phys. Control. Fusion 62 (4) (2020) 045007.
[24] S. Barzegar, A.R. Niknam, Laser pulse-electron beam synergy effect on electron self-injection and higher energy gain in laser wakefield accelerators, Sci. Rep. 11 (1) (2021) 37.
[25] A. Jain, D.N. Gupta, Improvement of electron beam quality in laser wakefield acceleration by a circularly-polarized laser pulse, Plasma Phys. Control. Fusion 63 (7) (2021) 075007.
[26] Y. Kitagawa, T. Matsumoto, T. Minamihata, et al., Beat-wave excitation of plasma wave and observation of accelerated electrons, Phys. Rev. Lett. 68 (1) (1992) 48.
[27] S.Ya. Tochitsky, R. Narang, C.V. Filip, et al., Enhanced acceleration of injected electrons in a laser-beat-wave-induced plasma channel, Phys. Rev. Lett. 92 (9) (2004) 095004.
[28] F. Amiranoff, J. Ardonceau, M. Bercher, et al., The plasma beat-wave acceleration experiment at Ecole Polytechnique, 363 (3) (1995) 497–510.
[29] M. Sedaghat, M. Ettehadi-Abari, B. Shokri, et al., The effect of external magnetic field on the bremsstrahlung nonlinear absorption mechanism in the interaction of high intensity short laser pulse with collisional underdense plasma, Phys. Plasmas 22 (3) (2015) 033114.
[30] M. Ettehadi-Abari, M. Sedaghat, B. Shokri, et al., Absorption of short laser pulses in underdense plasma by considering ohmic heating and ponderomotive force effects, Plasma Phys. Control. Fusion 57 (8) (2015) 08500.
[31] M. Kaur, D.N. Gupta, Simulation of laser-driven plasma beat-wave propagation in collisional weakly relativistic plasmas, Europhys. Lett. 116 (3) (2016) 35001.
[32] C.E. Clayton, C. Joshi, C. Darrow, et al., Relativistic plasma-wave excitation by collinear optical mixing, Phys. Rev. Lett. 54 (21) (1985) 2343.
[33] J. Cowley, C. Thornton, C. Arran, et al., Excitation and control of plasma wakefields by multiple laser pulses, 119 (4) (2017) 044802.
[34] W.P. Leemans, C.W. Siders, E. Esarey, et al., Plasma guiding and wakefield generation for second-generation experiments, IEEE Trans. Plasma Sci. 24 (2) (1996) 331–342.
[35] B. Sharma, A. Jain, N.K. Jaiman, et al., Laser pulse propagation in inhomogeneous magnetoplasma channels and wakefield acceleration, Phys. Plasmas 21 (2) (2014) 023108201.
[36] D.N. Gupta, M.R. Islam, D.G. Jang, et al., Self-focusing of a highintensity laser in a collisional plasma under weak relativistic-ponderomotive nonlinearity, Phys. Plasmas 20 (12) (2013) 123103.
[37] A.R. Niknam, S. Barzegar, M. Hashemzadeh, Self-focusing and stimulated Brillouin back-scattering of a long intense laser pulse in a finite temperature relativistic plasma, Phys. Plasmas 20 (12) (2013) 122117.
[38] A.J. Gonsalves, K. Nakamura, J. Daniels, et al., Petawatt laser guiding and electron beam acceleration to 8 GeV in a laser-heated capillary discharge waveguide, Phys. Rev. Lett. 122 (8) (2019) 084801.
[39] W.P. Leemans, A.J. Gonsalves, H.S. Mao, et al., Multi-GeV electron beams from capillary-discharge-guided subpetawatt laser pulses in the self-trapping regime, Phys. Rev. Lett. 113 (24) (2014) 245002.
[40] T.P.A. Ibbotson, N. Bourgeois, T.P. Rowlands-Rees, et al., Laser-wakefield acceleration of electron beams in a low density plasma channel, Phys. Rev. Spec. Top., Accel. Beams 13 (3) (2010) 031301.
[41] M. Ghorbanalilu, Focusing of intense laser beam by a thin axially magnetized plasma lens, Phys. Plasmas 17 (2) (2010) 023111.
[42] M. Ghorbanalilu, Axially magnetized electron positron and electron plasma competition on the self focusing of intense laser beam, Opt. Commun. 258 (5) (2012) 669–672.
[43] G. Shvets, X. Li, Theory of laser wakes in plasma channels, Phys. Plasmas 6 (2) (1999) 591–602.
[44] P. Sprangle, B. Hafizi, J.R. Penano, et al., Wakefield generation and GeV acceleration in tapered, Phys. Rev. E 63 (5) (2001) 056405.
[45] B. Hafizi, A. Ting, R.F. Hubbard, et al., Relativistic effects on intense laser beam propagation in plasma channels, Phys. Plasmas 10 (5) (2003) 1483.
[46] N.E. Andreev, L.M. Gorbunov, V.I. Kirsanov, et al., Structure of the wake field in plasma channels, Phys. Plasmas 4 (4) (1997) 1145–1153.
[47] M. Ghorbanalilu, Second and third harmonics generation in the interaction of strongly magnetized dense plasma with an intense laser beam, Laser Part. Beams 30 (2) (2012) 291–298.
[48] T.C. Wilson, F.Y. Li, M. Weikum, et al., Influence of strong magnetic fields on laser pulse propagation in underdense plasma, Plasma Phys. Control. Fusion 59 (6) (2017) 065002.
[49] G.D. Tsakiris, C. Gahn, V.K. Tripathi, Laser induced electron acceleration in the presence of static electric and magnetic fields in a plasma, Phys. Plasmas 7 (7) (2000) 3017–3030.
[50] C.T. Chiou, T. Katsouleas, C. Decker, et al., Laser wake-field acceleration and optical guiding in a hollow plasma channel, Phys. Plasmas 2 (1) (1995) 310–318.
[51] M. Sedaghat, S. Barzegar, A.R. Niknam, Quasi-phase-matched laser wakefield acceleration of electrons in an axially density-modulated plasma channel, Sci. Rep. 11 (1) (2021) 15207.
[52] W.H. Press, Integration of ordinary differential equations, in: Numerical Recipes in PASCAL, 1989.
[53] M. Arefnia, M. Ghorbanalilu, A.R. Niknam, Excitation and enhancement of wakefield by beating of two laser beams in a preformed plasma channel: an analytical study, Phys. Plasmas 29 (7) (2022) 072305.
[54] M.N. Sadiku, Numerical Techniques in Electromagnetics, CRC Press, 2000.
[55] M.S. Kim, D.G. Jang, T.H. Lee, I.H. Nam, I.W. Lee, H. Suk, Characteristics of a tapered capillary plasma waveguide for laser wakefield acceleration, Appl. Phys. Lett. 102 (20) (2013) 204103.
[56] J. Kim, V.L.J. Phung, K. Roh, M. Kim, K. Kang, H. Suk, Development of a density-tapered capillary gas cell for laser wakefield acceleration, Rev. Sci. Instrum. 92 (2) (2021) 02351.
[57] M. Rondanini, C. Cavallotti, D. Ricci, et al., An experimental and theoretical investigation of a magnetically confined dc plasma discharge, Rev. Sci. Instrum. 104 (1) (2008) 013304.
[58] T. Moscicki, J. Hoffman, Z. Szymanski, Laser ablation in an ambient gas: modelling and experiment, J. Appl. Phys. 123 (8) (2018) 083305.
[59] M. Turner, A.J. Gonsalves, S.S. Bulanov, et al., Radial density profile and stability of capillary discharge plasma waveguides of lengths up to 40 cm, High Power Laser Sci. Eng. 9 (2021) e17.
[60] E. Esarey, A. Ting, P. Sprangle, Optical guiding and beat wave phase velocity control in themplasma beat wave accelerator, AIP Conf. Proc. 193 (1) (1989) 71–86.
[61] M. Luo, C. Riconda, I. Pusztai, A. Grassi, J.S. Wurtele, T. Fülöp, Control of autoresonant plasma beat-wave wakefield excitation, Phys. Rev. Res. 6 (2024) 013338.
[62] A. Pukhov, N. Andreev, et al., Laser plasma wake velocity control by multi-mode beatwave excitation in a channel, Plasma 6 (1) (2023) 29.
[63] N.E. Andreev, S.V. Kuznetsov, et al., Monoenergetic laser wakefield acceleration, Phys. Rev. Spec. Top., Accel. Beams 3 (2) (2000) 021301.
[64] C.E. Clayton, K.A. Marsh, A. Dyson, et al., Ultrahigh-gradient acceleration of injected electrons by laser-excited relativistic electron plasma waves, Phys. Rev. Lett. 70 (1) (1993) 37.

[65] L.A. Gizzi, E. Boella, et al., Enhanced laser-driven proton acceleration via improved fast electron heating in a controlled pre-plasma, Sci. Rep. 11 (1) (2021).
[66] L.L. Ji, J. Snyder, et al., Towards manipulating relativistic laser pulses with micro-tube plasma lenses, Sci. Rep. 6 (1) (2016) 23256.
[67] J. Snyder, J. Snyder, et al., Relativistic laser driven electron accelerator using micro-channel plasma targets, Phys. Plasmas 26 (3) (2019).
[68] M.S. Hur, D.N. Gupta, H. Suk, Enhanced electron trapping by a static longitudinal magnetic field in laser wakefield acceleration, Phys. Lett. A 372 (15) (2008) 2684–2687.
[69] B. Nikrah, S. Jafari, Laser wakefield acceleration of electrons in a magnetically controlled plasma, Plasma Phys. Control. Fusion 65 (11) (2023) 115008.
[70] K. Bennett, Ch. Brady, H. Schmitz, et al., Users Manual for the EPOCH PIC Codes, University of Warwick, 2017.
[71] Z. Zhang, B. Zhu, Y. Li, et al., Generation of strong magnetic fields with a laser-driven coil, High Power Laser Sci. Eng. 6 (2018) e38.